NANO LETTERS

pubs.acs.org/NanoLett

Maskless Nanoscale Writing of Nanoparticle–Polymer Composites and Nanoparticle Assemblies using Thermal Nanoprobes

Woo Kyung Lee,[†] Zhenting Dai,[‡] William P. King,[‡] and Paul E. Sheehan*[,†]

[†]Code 6177, Chemistry Division, U.S. Naval Research Laboratory, Washington, D.C. 20375 and [‡]Department of Mechanical Science and Engineering, University of Illinois Urbana–Champaign, Urbana, Illinois 61801

ABSTRACT Nanoparticle polymer composites containing metal, semiconductor, magnetic, and optically active nanoparticles were deposited onto multiple substrates from a heatable atomic force microscope tip. The nanoparticle nanostructures were functional as deposited or could be etched with an oxygen plasma, revealing single nanoparticle lithographic resolution. Many types of nanoparticles can be patterned with the same technique, without the need to tailor the substrate chemistry and without solution processing.

KEYWORDS Nanolithography, nanocomposites, atomic force microscopy

Many creative approaches have been developed to fabricate nanostructures from nanoparticles[1–5] or nanoparticle composites,[6] but there are also many common limitations. In particular, most nanolithographies are developed for a particular material and require significant development for each new material or component. The required work for each new material significantly hinders fabricating devices that require multiple materials. A second hindrance is that many approaches for nanoparticle nanomanufacturing require prior deposition of a template or that the material first be deposited and then selectively removed.[7–9] With polymers, these multiple processing steps or sequential depositions can generate cross-contamination or degrade previously deposited structures. This paper reports additive maskless deposition of a wide range of nanoparticle types on multiple substrates with no solution processing and no sources of cross-contamination. This robust technique enables direct access to the exceptional properties of nanocomposites that promise significant advances in nanoelectronics,[10] data storage,[11] biosensors,[12,13] mechanics,[14] and optical imaging applications.[15]

Thermally controlled deposition from a heated tip, known as thermal dip-pen nanolithography (tDPN),[16] can deposit nanoscale quantities of materials that are otherwise difficult to deposit directly such as metals[17] and polymers.[18,19] In tDPN a heated atomic force microscope (AFM) probe tip[20] melts a solid ink and then directs the ink flow onto a surface. Adjusting tip temperature or speed allows deposition to be switched on or off and can precisely control feature dimensions. In the present paper, we show that the tDPN technique can be extended to nanocomposites with lithographic features having sub-100-nm width (Figure 1). Critically, to demonstrate the flexibility of the technique, we deposit with nanoscale precision a wide range of polymers that contain organometallic molecules or metallic, semiconducting, or magnetic nanoparticles (Figure 2 and Table 1) on several common AFM substrates—gold, mica, and silicon oxide (see Supporting Information). For all polymer–nanoparticle combinations, the ink was prepared and loaded onto the tip using the same dip-coating method described with the only variable being the cosolvent.

Thermally controlled deposition is ideal for depositing polymer nanocomposites since polymer melt processing provides more uniform and dense films[21] and more stable dispersion of the nanoparticles (nPs) in the polymer than those processed by solvents.[22] Moreover, our nanolithography approach is additive, is maskless, can deposit multiple

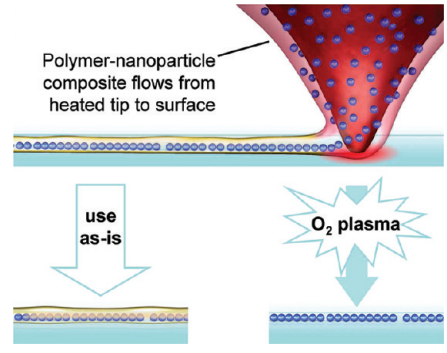

FIGURE 1. A polymer–nanoparticle composite is deposited from a heated cantilever tip. The deposited composite may be used as is or the polymer removed with an oxygen plasma. The nanoparticles can be either focused into a row or dispersed depending on the size and chemical treatment of the nanoparticles.

* To whom correspondence should be addressed: paul.sheehan@nrl.navy.mil; phone, 202.404.3386.

Received for review: 09/14/2009
Published on Web: 00/00/0000

DOI: 10.1021/nl9030456 | *Nano Lett.* **XXXX,** *xxx,* 000-000

Report Documentation Page

Form Approved
OMB No. 0704-0188

1. REPORT DATE	2. REPORT TYPE	3. DATES COVERED
SEP 2009		**00-00-2009 to 00-00-2009**

4. TITLE AND SUBTITLE	5a. CONTRACT NUMBER
Maskless Nanoscale Writing of Nanoparticle-Polymer Composites and Nanoparticle Assemblies using Thermal Nanoprobes	5b. GRANT NUMBER
	5c. PROGRAM ELEMENT NUMBER
6. AUTHOR(S)	5d. PROJECT NUMBER
	5e. TASK NUMBER
	5f. WORK UNIT NUMBER
7. PERFORMING ORGANIZATION NAME(S) AND ADDRESS(ES) **Naval Research Laboratory,Code 6177, Chemistry Division,Washington,DC,20375**	8. PERFORMING ORGANIZATION REPORT NUMBER
9. SPONSORING/MONITORING AGENCY NAME(S) AND ADDRESS(ES)	10. SPONSOR/MONITOR'S ACRONYM(S)
	11. SPONSOR/MONITOR'S REPORT NUMBER(S)

12. DISTRIBUTION/AVAILABILITY STATEMENT
Approved for public release; distribution unlimited

13. SUPPLEMENTARY NOTES

14. ABSTRACT
see report

15. SUBJECT TERMS

16. SECURITY CLASSIFICATION OF:			17. LIMITATION OF ABSTRACT	18. NUMBER OF PAGES	19a. NAME OF RESPONSIBLE PERSON
a. REPORT	b. ABSTRACT	c. THIS PAGE			
unclassified	**unclassified**	**unclassified**	**Same as Report (SAR)**	**5**	

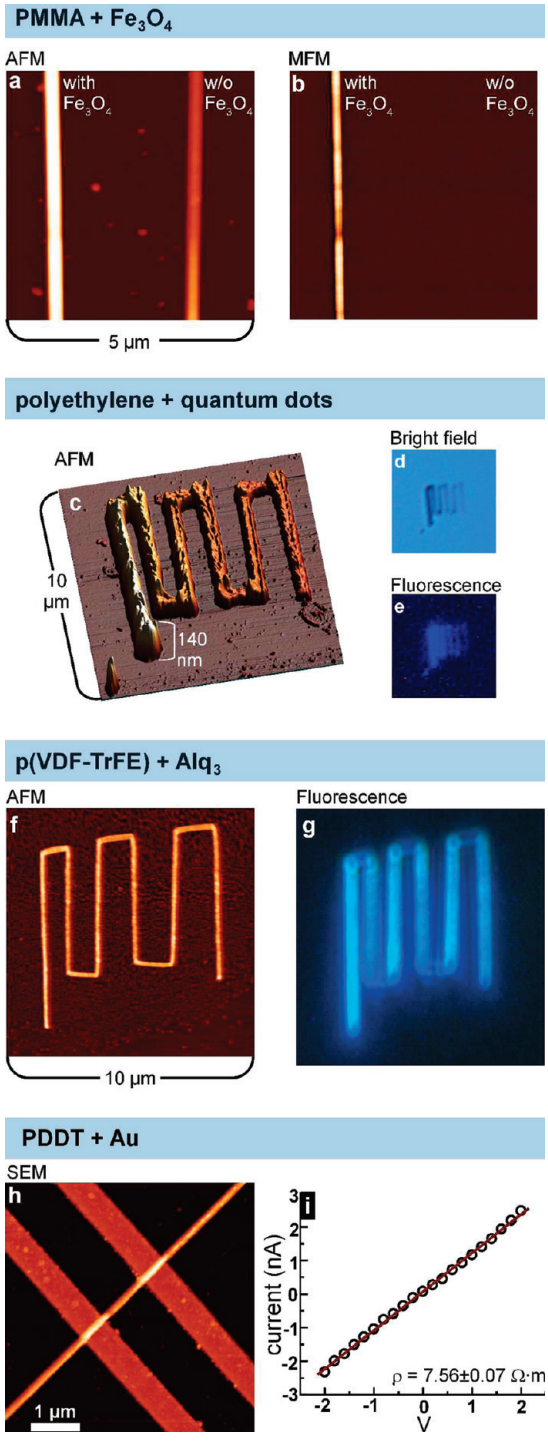

FIGURE 2. The deposited polymer/nanoparticle or small molecule via tDPN and its own properties. (a) The topography of two lines of PMMA only one of which contains iron oxide nanoparticles. (b) Magnetic Force Microscope image of the same showing that only the structure that contains the iron oxide particles is magnetically active. (c–e) AFM of a polyethylene/QD composite showing the fluorescence of the deposited structure. (f, g) Deposition of the otherwise difficult to deposit Alq_3 using a p(VDF-TrFE) carrier. The Alq_3 retains its ability to fluoresce after deposition. (h) SEM of the conductive polymer poly(3-dodecylthiophene) (PDDT) with 5.0% by volume Au nPs deposited across Au electrodes. (i) $I-V$ plot from a two-probe measurement of the PDDT–Au composite. Together, these show that tDPN is a robust method for depositing many different polymer composites.

nanocomposites, and is not substrate specific. The deposition process may be illustrated using the polymer poly(methyl methacrylate) (PMMA). PMMA is an excellent nanocomposite matrix since it flows well and since it mixes well with many inorganic nPs due to the adhesion of its side chains to the hydroxyl groups of metal oxide nPs.[23] PMMA is also ideal when acting merely as a carrier since it is readily etched using wet or dry techniques (parts a and b of Figure 3) or by thermal decomposition.[23–25] To make the ink, magnetic Fe_3O_4 nanoparticles (nucleus diameter 6.5 ± 3.0 nm) were codissolved with PMMA (MW = 50 kg/mol) in chloroform at 0.1% by volume and then ultrasonicated for 30 min to ensure uniform dispersion. A small metal loop would then hold a droplet of the ink solution while the cantilever is dipped into it. The coated probe tip could then directly deposit the nanocomposite onto different substrates (see Figure S1 in Supporting Information). By variation of the temperature and speed of the probe, the width of the deposited ink could be adjusted from 78 to 400 nm with comparable heights (see Figures S2e and S3 in Supporting Information).

To show that the nanoparticles remained functional after deposition, we deposited a line of pure PMMA next to a line of PMMA containing magnetic Fe_3O_4 nanoparticles. The magnetic response of Fe_3O_4 loaded polymer is clearly visible while, as expected, there is no magnetic response from the Fe_3O_4-free material (Figure 2b). Note that these figures also demonstrate the ease with which a new structure may be placed next to an existing one without degrading the prior's performance. We observed full functionality in all inks tested. Polyethylene with CdSe/ZnS quantum dots fluoresced due to the quantum dots as did the metallorganic tris(8-hydroxyquinolinato)aluminum mixed with the piezoelectric polymer P(VDF-TrFE) (Figure 2c–g). Finally, a two-probe conductivity measurement showed that the inclusion of Au nanoparticles reduced the resistivity of the otherwise undoped conductive polymer PDDT to $<7.56 \pm 0.07\ \Omega \cdot m$, a significant reduction from the intrinsic value[26] of 500 $k\Omega \cdot m$. The successful deposition of organometallic, oxide, semiconducting, and metallic nanoparticles demonstrates the flexibility of the technique.

The functional nanocomposite lines may be left as-deposited or the polymer matrix may be removed with an oxygen plasma leaving just the nanoparticles. While analyzing the residual Fe_3O_4 nPs deposited with PMMA, it was found that the nPs had formed rows significantly narrower than the overall deposit. Parts a–c of Figure 3 show the dramatic reduction in line width when a PMMA/Fe_3O_4 composite was plasma etched to remove the PMMA thereby revealing a row of nanoparticles 10 nm wide. The plasma processing reduced the deposit cross sectional area by a factor of 993 which, when compared to the 0.1% particle loading, indicates that essentially all the nanoparticles are driven to the center line. From a nanolithography standpoint, the more critical aspect is that the line width shrinks

DOI: 10.1021/nl9030456 | *Nano Lett.* **XXXX,** *xxx,* 000-000

TABLE 1. Example Nanoparticle Inks Deposited from a Heated Tip

particle/metallorganic	nP diameter (nm)	polymer	W_{total}/W_{nP}
aluminum tris(8-hydroxyquinoline) (Alq_3)	~0.9	P(VDF-TrFE)	1
zinc diethyldithiocarbamate	~1.2	P(VDF-TrFE)	1
CdSe-ZnS core−shell	2−4	PE	1
dodecanethiol functionalized silver	2−4	PMMA	n/m
dodecanethiol functionalized gold	2−4	PMMA	1.9
		PDDT	1.5
HMDS-functionalized Fe_3O_4	6	PMMA	2.3
Fe_3O_4	6.5 ± 3.0	PMMA	36

a factor of 36 from 360 to 10 nm (Figure 3c). We refer to this enhancement of the nanoparticle concentration at the center of the deposit as "focusing". Table 1 shows several material systems that we have patterned and includes the ratio of nP row width, w_{nP}, to nanocomposite widths, w_{total}. The results reveal two trends in focusing. The first trend is that the nPs coated with a layer that interacts strongly with the polymer are more focused. This is seen most clearly when the highly focusing Fe_3O_4 nanoparticles were functionalized with hexamethyldisilazane (HMDS) to leave an alkyl termination that interacts poorly with the polymer. These treated nanoparticles are focused from an initial nanocomposite line width of 439 nm to a postplasma etch width of 187 nm, which is only a factor of 2.3× and significantly less than the prior 36×. The second trend is that larger particles tend to be more readily focused. For instance the Au nPs with a diameter of 2−4 nm are focused from a width of 470 nm to a width of 250 nm, or a factor of 1.9, a small decrease from the HMDS functionalized Fe_3O_4 nPs.

Since the particles are focused before etching (Figure 4d), focusing must occur during deposition. The most probable alignment mechanism is the shearing of the polymer matrix during deposition. Nanoparticle alignment due to matrix shearing has been previously observed at the macroscale[27−29] with comparable shear rates of 10−100 s^{-1}. In those works it was shown that alignment depended on the balance between diffusion which dispersed the nanoparticles and advection in the shear flow which aligned the nPs. The relative dominance of one of these two effects is conveyed by the Péclet number $Pe = \dot{\gamma}\eta_E r^3/k_B T$, where $\dot{\gamma}$ is the shear rate, η_E is the shear viscosity at experimental conditions, and r is the nP radius, with lower (<1) Péclet numbers indicating the dominance of diffusion. Thus, for the 1 nm metallorganics, $Pe \sim 0.01$ indicating the predominance of diffusion and therefore even dispersion. For the 6.5 nm diameter Fe_3O_4 nPs $Pe \sim 2$ indicated that shear alignment of the nPs is predominant (see Supporting Information). Alignment will also depend on the local viscosity η_E which depends strongly on the nP's surface functionalization. Poorly interacting nPs have less viscous interlayers that allow the polymer chains to slip around instead of orient the nPs and so are less efficiently aligned by the polymer. This will be reflected in a lower viscosity which in turn will lower Pe. Finally, shear-induced alignment is consistent with the clustering of the nanoparticles when the tip does not move (Figure 4a−c). Experiments were limited in part by the commercial availability of the nPs of defined diameter and functionality. Of particular interest will be testing the strong cubic dependency of Pe on the nP radius. Future examination of sets of homologous nPs of controlled diameter will further test the proposed alignment mechanism and potentially provide a pathway to focusing even smaller nanoparticles.

This nanolithography has both advantages and apparent limitations. This approach is maskless, patterns additively, avoids solution processing, and is exceptionally flexible in the range of materials easily deposited. It is also achieves line widths for both the nP rows and the nanocomposite nanostructures that are much narrower than those in previous reports of directly written structures. For instance, fabrication of gold nanoparticle patterns by nanoimprint lithography has been developed; however, the line width was >130 nm.[1,30] Conventional DPN has been used to directly deposit functionalized gold nanoparticles by electrostatic interaction from single nanoparticles to its aggregates, but again line widths generally exceed 100 nm.[31,32] Recently, Wang et al.[32] showed that DPN could deposit rows of Au nPs that were roughly one nP wide (actual widths not reported); however, deposition was inhomogeneous leading to start-and-stop deposition. The present technique has limitations as well. The loading of the nanoparticle into the polymer should be thermodynamically stable in the polymer which requires tuning the sizes and chemistries of the polymer and nanoparticles.[22] For instance, it is known that the dispersion of nanoparticles in a polymer matrix is not thermodynamically stable if the nP's radius exceeds the polymer's radius of gyration (R_g), indeed, a limitation of this technique is that it could not deposit nanoparticles whose radii exceeded the R_g (~6 nm)[33] of the PMMA. Consequently, deposition of larger nPs would require higher molecular weight inks or covalent linkage of the nPs to the polymer. Second, the addition of high concentrations of nPs increases the ink viscosity and thereby slows deposition. Whereas tDPN can normally write pure polymers up to ~200 μm/s, the writing speed for nanocomposites is somewhat less at <2 μm/s, though this remains significantly faster than conventional DPN of polymers due to the increased polymer mobility in the melt. Finally, if the goal is complete dispersion of the nanoparticles in a single pass, then the nP size and functionality should be adjusted appropriately.

In summary, this paper reports that thermal deposition is a generic strategy for depositing a wide range of nanocomposites that may be used as is or modified to leave dense

DOI: 10.1021/nl9030456 | *Nano Lett.* **XXXX,** *xxx,* 000-000

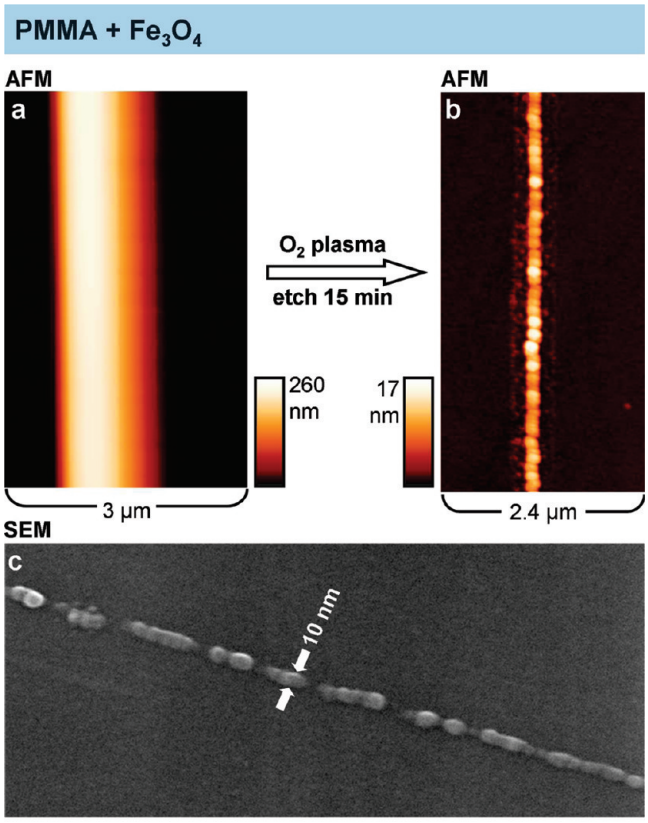

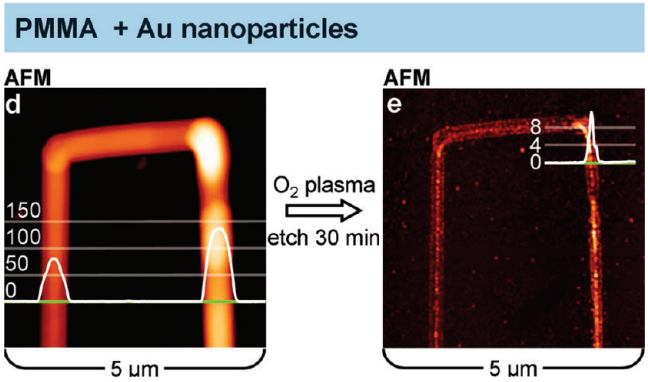

FIGURE 3. (a) AFM topographs a 400 nm wide (fwhm) PMMA line via tDPN. (b) The same structure after exposure to 135 W oxygen rf plasma for 15 min. The average height of the row is 8 nm indicating single particles. Note that the finite size of the AFM probe increases the apparent width of the particles. (c) SEM of the plasma cleaned particles showing the 10 nm wide lines. (d) AFM of a PMMA line written at 1.0 μm/s (left), 1.0 μm/s (top), and 0.5 μm/s (right). (e) After plasma etching the Au nanoparticles are revealed showing line widths of 250 nm. This focusing is less than that for Fe_3O_4 nanoparticles after plasma etching.

rows of nanoparticles. We successfully deposited on many substrates of interest for optics, electronics, and biology. Moreover, to the best of our knowledge, we report the smallest line widths achieved for directly deposited materials for both nanoparticles rows (10 nm) and nanoparticle–polymer composites (78 nm). Shear flow induced focusing should allow resolutions limited mainly by nanoparticle size and polymer molecular weight.

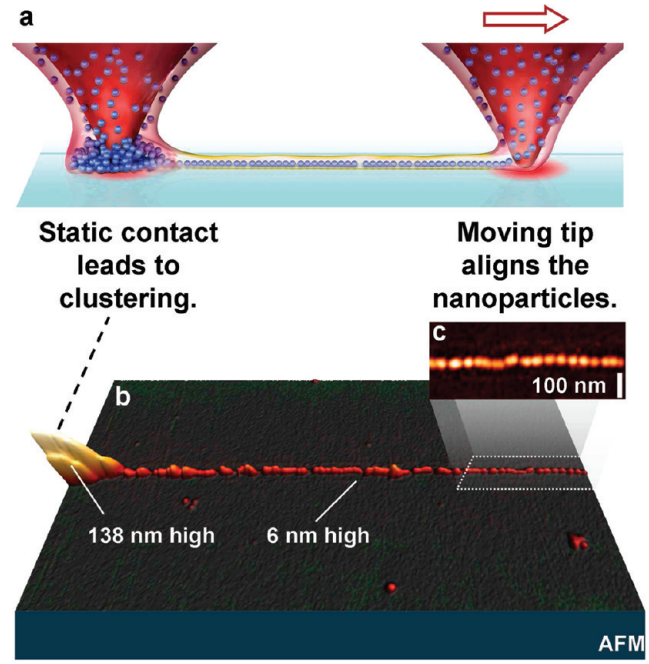

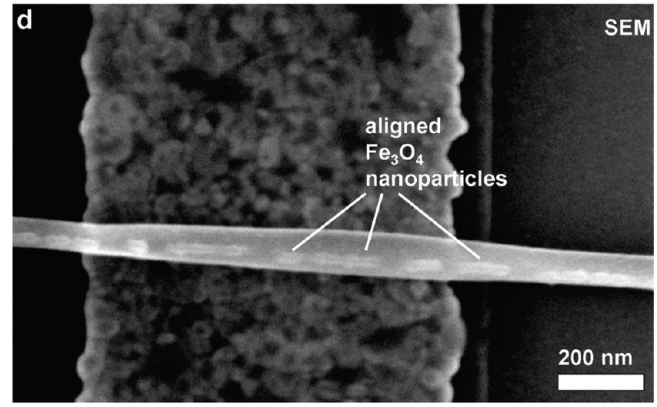

FIGURE 4. Schematic diagram of PMMA–Fe_3O_4 nanoparticles' deposition and focusing. (a) Nanoparticles condense onto the tip during deposition. When the tip is still, nanoparticles will build up while moving the tip aligns the nanoparticles. (b) Fe_3O_4 nanoparticles clustered when the tip was held still for 2 s and were aligned into a row of single nanoparticles when the tip was moved. (c) A top view of the aligned nanoparticles. (d) Large, HMDS-modified nanoparticles are partially aligned in PMMA deposited across an electrode (see Supporting Information).

Acknowledgment. The authors are grateful for funding from the DARPA TBN program, ONR Nanoelectronics, and the NSF Center for Nanoscale Chemical-Electro-Mechanical Manufacturing Systems (Nano-CEMMS). W.K.L. thanks the National Research Council for support of his postdoctoral research.

Supporting Information Available. Descriptions of ink preparation, cantilever heating calibration, ink viscosity calculation, and deposition on multiple substrates.This material is available free of charge via the Internet at http://pubs.acs.org.

DOI: 10.1021/nl9030456 | *Nano Lett.* **XXXX,** *xxx,* 000-000

REFERENCES AND NOTES

(1) Ko, S. H.; Park, I.; Pan, H.; Grigoropoulos, C. P.; Pisano, A. P.; Luscombe, C. K.; Frechet, J. M. J. *Nano Lett.* **2007**, *7*, 1869–1877.
(2) Kinge, S.; Crego-Calama, M.; Reinhoudt, D. N. *ChemPhysChem* **2008**, *9*, 20–42.
(3) Tang, Z. Y.; Kotov, N. A. *Adv. Mater.* **2005**, *17*, 951–962.
(4) Maury, P.; Escalante, M.; Reinhoudt, D. N.; Huskens, J. *Adv. Mater.* **2005**, *17*, 2718.
(5) Zhang, G.; Wang, D. Y.; Mohwald, H. *Nano Lett.* **2007**, *7*, 127–132.
(6) Shenhar, R.; Norsten, T. B.; Rotello, V. M. *Adv. Mater.* **2005**, *17*, 657–669.
(7) Lee, W. K.; Sheehan, P. E. *Scanning* **2008**, *30*, 172–183.
(8) Nie, Z. H.; Kumacheva, E. *Nat. Mater.* **2008**, *7*, 277–290.
(9) Salaita, K.; Wang, Y. H.; Mirkin, C. A. *Nat. Nanotechnol.* **2007**, *2*, 145–155.
(10) Dadosh, T.; Gordin, Y.; Krahne, R.; Khivrich, I.; Mahalu, D.; Frydman, V.; Sperling, J.; Yacoby, A.; Bar-Joseph, I. *Nature* **2005**, *436*, 677–680.
(11) Sun, S. H.; Murray, C. B.; Weller, D.; Folks, L.; Moser, A. *Science* **2000**, *287*, 1989–1992.
(12) Bruchez, M.; Moronne, M.; Gin, P.; Weiss, S.; Alivisatos, A. P. *Science* **1998**, *281*, 2013–2016.
(13) Elghanian, R.; Storhoff, J. J.; Mucic, R. C.; Letsinger, R. L.; Mirkin, C. A. *Science* **1997**, *277*, 1078–1081.
(14) Liff, S. M.; Kumar, N.; McKinley, G. H. *Nat. Mater.* **2007**, *6*, 76–83.
(15) Nie, S. M.; Emery, S. R. *Science* **1997**, *275*, 1102–1106.
(16) Sheehan, P. E.; Whitman, L. J.; King, W. P.; Nelson, B. A. *Appl. Phys. Lett.* **2004**, *85*, 1589.
(17) Nelson, B. A.; King, W. P.; Laracuente, A. R.; Sheehan, P. E.; Whitman, L. J. *Appl. Phys. Lett.* **2006**, 88.
(18) Lee, W. K.; Whitman, L. J.; Lee, J.; King, W. P.; Sheehan, P. E. *Soft Matter* **2008**, *4*, 1844.
(19) Yang, M.; Sheehan, P. E.; King, W. P.; Whitman, L. J. *J. Am. Chem. Soc.* **2006**, *128*, 6774.
(20) Lee, J.; Beechem, T.; Wright, T. L.; Nelson, B. A.; Graham, S.; King, W. P. *J. Microelectromech. Syst.* **2006**, *15*, 1644.
(21) Luzinov, I.; Julthongpiput, D.; Malz, H.; Pionteck, J.; Tsukruk, V. V. *Macromolecules* **2000**, *33*, 1043.
(22) Mackay, M. E.; Tuteja, A.; Duxbury, P. M.; Hawker, C. J.; Van Horn, B.; Guan, Z. B.; Chen, G. H.; Krishnan, R. S. *Science* **2006**, *311*, 1740–1743.
(23) Rittigstein, P.; Priestley, R. D.; Broadbelt, L. J.; Torkelson, J. M. *Nat. Mater.* **2007**, *6*, 278–282.
(24) Baker, C.; Shah, S. I.; Hasanain, S. K. *J. Magn. Magn. Mater.* **2004**, *280*, 412–418.
(25) Kotlyar, A.; Perkas, N.; Amiryan, G.; Meyer, M.; Zimmermann, W.; Gedanken, A. *J. Appl. Polym. Sci.* **2007**, *104*, 2868–2876.
(26) Yoshino, K.; Park, D. H.; Park, B. K.; Onoda, M.; Sugimoto, R. *Jpn. J. Appl. Phys.* **1988**, *27*, No. L1612—L1615.
(27) Brickweg, L. J.; Floryancic, B. R.; Sapper, E. D.; Fernando, R. H. *J. Coat. Technol. Res.* **2007**, *4*, 107–110.
(28) Ackerson, B. J.; Pusey, P. N. *Phys. Rev. Lett.* **1988**, *61*, 1033–1036.
(29) Ackerson, B. J. *J. Rheol.* **1990**, *34*, 553–590.
(30) Park, I.; Ko, S. H.; Pan, H.; Grigoropoulos, C. P.; Pisano, A. P.; Frechet, J. M. J.; Lee, E. S.; Jeong, J. H. *Adv. Mater.* **2008**, *20*, 489–496.
(31) Wang, H. T.; Nafday, O. A.; Haaheim, J. R.; Tevaarwerk, E.; Amro, N. A.; Sanedrin, R. G.; Chang, C. Y.; Ren, F.; Pearton, S. J. *Appl. Phys. Lett.* **2008**, 93.
(32) Wang, W. C. M.; Stoltenberg, R. M.; Liu, S. H.; Bao, Z. N. *ACS Nano* **2008**, *2*, 2135–2142.
(33) Fetters, L. J.; Lohse, D. J.; Richter, D.; Witten, T. A.; Zirkel, A. *Macromolecules* **1994**, *27*, 4639–4647.

DOI: 10.1021/nl9030456 | *Nano Lett.* **XXXX,** *xxx,* 000-000